

# Ground Non-Linearity Calibration

F. Masci, 5/5/2009, v. 2.0

## 1. Summary

Below we summarize our analysis of Sample-Up-the-Ramp (SUR) data from the FEB taken during the first MIC2 test for calibrating the non-linearity. Flight Model (FM) test data was acquired on 11-12-2008 and Engineering Model (EM) data on 11-19-2008.

Here's a summary of the delivered products:

```
gndlincal-w1-est-v2.fits  
gndlincal-w1-msk-v2.fits  
gndlincal-w1-unc-v2.fits
```

```
gndlincal-w2-est-v2.fits  
gndlincal-w2-msk-v2.fits  
gndlincal-w2-unc-v2.fits
```

```
gndlincal-w3-est-v2.fits  
gndlincal-w3-msk-v2.fits  
gndlincal-w3-unc-v2.fits
```

```
gndlincal-w4-est-v2.fits  
gndlincal-w4-msk-v2.fits  
gndlincal-w4-unc-v2.fits
```

where “est” = estimate of non-linearity (quadratic) coefficient; “msk” = calibration mask indicating highly non-linear, very uncertain, and bad ramp-fit pixels; “unc” = 1-sigma uncertainty in non-linearity coefficient.

All the above used the FM electronics data at nominal temperature (as defined at the time - see below). Non-linearity estimates using the EM data are very close to those from FM, albeit slightly smaller (or less non-linear) across all bands: cf. Tables 1 and 2. This could be due to the difference in array temperatures.

**NOTE:** Version 1 of the calibration products used method 1 (as described below). Version 2 uses the more reliable method 2 and the calibration products have been replaced.

This document is organized as follows:

**Section 2:** Non-linearity Models

**Section 3:** Analysis Method

**Section 4:** Results Summary

**Section 5:** Masking Criteria

**Section 6:** Conclusions

**Section 7:** Diagnostic Plots (all bands)

## 2. Non-linearity Models

### Method 1: fitting SUR data at a single fixed illumination close to A/D saturation

An initial analysis of the FEB data for a few pixels revealed that a quadratic correction model was sufficient. This model and the method that uses it was found to be adequate for the *Spitzer* MIPS arrays. The method is based on first fitting the lab SUR data with the following model:

$$y_i = \alpha i^2 + \beta i, \quad (\text{Eq. 1})$$

where

$y_i$  = measured SUR value at sample  $i = 0, 1, 2 \dots 8$ , and  $\alpha, \beta$  are the fit coefficients.

It is assumed that the SUR data has been zero-baselined so that no intercept is required, i.e.,  $y_0 = 0$ . The ramp intercept at the zeroth sample plays no role in determining the ramp shape.

The parameters  $\alpha$  and  $\beta$  are estimated by fitting Eq. 1 to the ramp data  $y_i$  for each pixel using  $\chi^2$  minimization. The quantity to be minimized is:

$$\chi^2 = \sum_i^N \frac{[y_i - (\alpha i^2 + \beta i)]^2}{\sigma_i^2}, \quad (\text{Eq. 2})$$

where  $\sigma_i$  are estimates of the uncertainties, e.g., the RMS of repeated exposures from the mean at each ramp sample. Since Eq. 1 is linear in the coefficients, the values of  $\alpha$  and  $\beta$  that minimize  $\chi^2$  can be written in closed form:

$$\alpha = \frac{K_2 K_5 - K_3 K_4}{K_2^2 - K_1 K_4} \quad (\text{Eq.3})$$

$$\beta = \frac{K_2 K_3 - K_1 K_5}{K_2^2 - K_1 K_4},$$

and the error-covariance matrix elements are given by:

$$\sigma_\alpha^2 = \frac{-K_4}{K_2^2 - K_1 K_4} \quad (\text{Eq.4})$$

$$\sigma_\beta^2 = \frac{-K_1}{K_2^2 - K_1 K_4}$$

$$\text{cov}(\alpha, \beta) = \frac{K_2}{K_2^2 - K_1 K_4},$$

where:

$$K_1 = \sum_i^N i^4 / \sigma_i^2$$

$$K_2 = \sum_i^N i^3 / \sigma_i^2$$

$$K_3 = \sum_i^N i^2 y_i / \sigma_i^2$$

$$K_4 = \sum_i^N i^2 / \sigma_i^2$$

$$K_5 = \sum_i^N i y_i / \sigma_i^2.$$

$N$  is the total number of data points in the fit and can include multiple ramps from repeated exposures at the *same* illumination.

Given that Eq. 1 is fit to specific lab calibration data, we can generalize to any other observed ramp with underlying *linear count rate*  $\beta_i$  by scaling the “time”  $i$  at which the linear counts are equal, i.e., if  $\beta_i = \beta_i'$  at times  $i$  and  $i'$ , then  $i = \beta_i' / \beta$ . We can then transform Eq. 1 into a new generic expression for the counts in a ramp with linear rate  $\beta_i$ .

$$y_{i'} = \left( \frac{\alpha}{\beta^2} \right) \beta_i^2 i'^2 + \beta_i i'. \tag{Eq. 5}$$

The assumption of this method should now be apparent: the quantity  $\alpha/\beta^2$  is assumed to be constant and independent of the incident flux. The parameter  $\alpha$  is  $< 0$  since non-linear ramps generally curve downwards. This means the fractional loss in the measured counts at any ramp sample  $i$  from the linear expectation is  $(\alpha/\beta^2)\beta_i i$ . A higher incident flux will therefore suffer a proportionally greater loss at all ramp samples.

The output signal from the DEB is computed on-board from the FEB SUR data  $y_i$  as:

$$m = \frac{1}{2^T} \left[ O + \sum_{i=0}^N c_i y_i \right], \tag{Eq. 6}$$

where nominally  $N = 8$  samples,  $O$  is an offset,  $c_i$  are the SUR weighting coefficients, and  $T$  is the number of LSBs truncated. A *linear* output signal from the DEB (i.e., assuming a detector was perfectly linear) can be written in terms of the true *linear* ramp count ( $\beta_i i$ ) and SUR coefficients using Eq. 6:

$$m_{lin} = \frac{1}{2^T} \left[ \sum_{i=0}^N c_i \beta_i i \right], \tag{Eq. 7}$$

where it is assumed that a dark along with the DEB bias ( $O/2^T$ ) has been removed. On re-arranging, the true linear rate can be written in terms of the linear DEB signal as follows:

$$\beta_l = \left( \frac{2^T}{\sum_{i=0}^N c_i i} \right) m_{lin}. \quad (\text{Eq. 8})$$

Substituting Eq. 8 into Eq. 5, we obtain:

$$y_i = \left( \frac{\alpha}{\beta^2} \right) \Omega^2 m_{lin}^2 i^2 + \Omega m_{lin} i, \quad (\text{Eq. 9})$$

where

$$\Omega = \frac{2^T}{\sum_{i=0}^N c_i i}.$$

Substituting Eq. 9 into the DEB formula (Eq. 6) and rearranging terms, the observed DEB value ( $m_{obs}$ ) for a pixel can be written in terms of its linearized counterpart ( $m_{lin}$ ) *after* subtraction of the dark and DEB bias ( $O/2^T$ ) as follows:

$$m_{obs} = C m_{lin}^2 + m_{lin}, \quad (\text{Eq. 10})$$

where

$$C = \frac{\alpha}{\beta^2} \frac{2^T \sum_{i=0}^N c_i i^2}{\left[ \sum_{i=0}^N c_i i \right]^2}. \quad (\text{Eq. 11})$$

Generally we expect  $C \leq 0$  with  $C = 0$  implying a perfectly linear response. The quantity  $C$  in Eq. 11 is defined as the non-linearity coefficient and is provided (along with its uncertainty and bad-calibration mask) as a FITS image for use in the instrumental calibration (ICAL) pipeline. The 1-sigma uncertainty in  $C$  uses the error-covariance matrix in the fit coefficients (Eq. 4). This can be written:

$$\sigma_C = C \left[ \frac{\sigma_\alpha^2}{\alpha^2} + \frac{4\sigma_\beta^2}{\beta^2} - \frac{4 \text{cov}(\alpha, \beta)}{\alpha\beta} \right]^{1/2}. \quad (\text{Eq. 12})$$

Eq. 10 can be inverted to solve for the linearized signal  $m_{lin}$ :

$$m_{lin} = \frac{2m_{obs}}{1 + \sqrt{1 + 4Cm_{obs}}} \quad \text{for } m_{obs} \leq m_{obs}(\text{max}) \leq -\frac{1}{4C}. \quad (\text{Eq. 13})$$

The quantity in the square root is the discriminant:

$$D = 1 + 4Cm_{obs}$$

and we require  $D \geq 0$  for a physical solution. This implies there is a maximum observed signal:  $m_{obs} = -1/(4C)$  above which a measurement cannot be linearized and hence could not have come from a detector with this non-linearity model. It is very possible that the signal predicted by Eq. 10 turns-over before the maximum of the DEB dynamic range is reached: 32752. Signals satisfying  $-1/(4C) < m_{obs} \leq 32752$  therefore cannot be linearized using this model. To avoid (or “soften” the impact of) a possible turn-over, we define the quadratic model solution in Eq. 13 to be only applicable to observed signals  $m_{obs} \leq m_{obs}(\max)$ , where  $m_{obs}(\max)$  is a new calibration parameter. For  $m_{obs} > m_{obs}(\max)$ , we Taylor expand Eq. 13 about  $m_{obs} = m_{obs}(\max)$  to first order and linearly extrapolate to estimate the linearized signal, i.e.:

$$m_{lin} \approx m_{lin}(\max) + [m_{obs} - m_{obs}(\max)] \left. \frac{\partial m_{lin}}{\partial m_{obs}} \right|_{m_{obs} = m_{obs}(\max)}$$

Using Eqs 10 and 13, the linearized signal for observed signals  $m_{obs} > m_{obs}(\max)$  can then be written:

$m_{lin} \approx m_{lin}(\max) + \frac{m_{obs} - m_{obs}(\max)}{2Cm_{lin}(\max) + 1} \quad \text{for } m_{obs} > m_{obs}(\max), \quad (\text{Eq. 14})$ <p>where</p> $m_{lin}(\max) = \frac{2m_{obs}(\max)}{1 + \sqrt{1 + 4Cm_{obs}(\max)}}.$
--

This extends the flexibility of the quadratic model and is important for characterizing the non-linearity at high observed signals where its effects are most extreme and there is no guarantee that it follows a pure quadratic. The only caveat is that it introduces a new parameter:  $m_{obs}(\max)$ . This can be determined graphically provided the calibration data span a large enough dynamic range.

The formalism for estimating uncertainties in linearized signals is described in the ICAL SDS document.

## **Method 2: fitting SUR data taken at a number of different illuminations spanning full dynamic range**

The above model derives a non-linearity coefficient (Eq. 11) for each pixel by fitting ramp data at a *single* ‘maximal’ (unsaturated) illumination and then assumes this holds at all other illuminations. Analysis has shown this to be approximately true on *Spitzer*, but it’s a dangerous assumption in general. The new method presented here removes this assumption and is believed to be more direct and trustworthy by the author. For the method to be reliable, we need good sampling of the illumination over the full observed (DEB) dynamic range.

This method still involves fitting a quadratic model to ramp data (for each pixel) using the formalism above, i.e., Eq. 1, except that now it is fit to data at each and every illumination level. This yields a set of “illumination-dependent” coefficients:  $(\alpha, \beta)_{I=1}$ ,  $(\alpha, \beta)_{I=2}$ ,  $(\alpha, \beta)_{I=3}$ , etc...

We recall the formula for the observed DEB signal in Eq. 6. After dark subtraction (and consequently removal of the offset  $O/2^T$ ) as performed in the ICAL pipeline, the observed signal can be written in terms of the fit coefficients at any illumination using Eq. 1:

$$m_{obs} = \frac{1}{2^T} \left[ \alpha \sum_{i=0}^N c_i i^2 + \beta \sum_{i=0}^N c_i i \right],$$

or

$$m_{obs} = \frac{\alpha}{2^T} \left[ \sum_{i=0}^N c_i i^2 \right] + m_{lin}, \quad (\text{Eq. 15})$$

where

$$m_{lin} = \frac{\beta}{2^T} \sum_{i=0}^N c_i i \quad (\text{Eq. 16})$$

For every illumination-dependent pair of coefficients  $(\alpha, \beta)_I$ , we compute corresponding pairs of linearized and (predicted) observed DEB signals  $(m_{lin}, m_{obs})_I$  using Eqs 16 and 15 respectively. A functional relation  $m_{obs} = f(m_{lin})$  is then fitted to all the  $(m_{lin}, m_{obs})$  data. We start with Eq. 10 and fit for the single parameter  $C$ . This function is an obvious choice since it was used to estimate the input data points  $(m_{lin}, m_{obs})_I$ . A direct fit to all the illumination dependent  $(m_{lin}, m_{obs})$  pairs then amounts to a refinement of  $C$  over that estimated from the ramp data at a single illumination. This fit uses the uncertainties in each of the  $(m_{lin}, m_{obs})_I$  and their covariance as propagated from the uncertainties in  $(\alpha, \beta)_I$ . The  $\chi^2$  metric to minimize is therefore more complicated:

$$\chi^2 = \sum_i^{N_I} \frac{\left[ m_{obsi} - (Cm_{mlini}^2 + m_{lini}) \right]^2}{\sigma_{mobsi}^2 - (2 + 4Cm_{lini}) \text{cov}(m_{lini}, m_{obsi}) + \sigma_{mlini}^2 (1 + 4Cm_{lini} + 4C^2 m_{mlini}^2)},$$

where the sum is over all the  $N_I$  illuminations [number of data pairs  $(m_{lin}, m_{obs})$ ] and

$$\sigma_{mobsi}^2 = K^2 \sigma_\alpha^2 + M^2 \sigma_\beta^2 + 2MK \text{cov}(\alpha, \beta);$$

$$\sigma_{mlini}^2 = M^2 \sigma_\beta^2;$$

$$\text{cov}(m_{lini}, m_{obsi}) = MK \text{cov}(\alpha, \beta) + 2M^2 \sigma_\beta^2;$$

$$K = \frac{1}{2^T} \sum_{i=0}^8 c_i i^2; \quad M = \frac{1}{2^T} \sum_{i=0}^8 c_i i.$$

The solution to  $\partial\chi^2/\partial C = 0$  is inherently non-linear, however, a linear approximation assuming  $\sigma_{mlini}^2 = 0$  and  $\text{cov}(m_{lini}, m_{obsi}) = 0$  can initially be used to get an estimate for  $C$  and its uncertainty. The uncertainty can be checked using a Monte-Carlo simulation and then rescaled if necessary. When  $C$  is obtained, it can be used in Eqs 13 and 14 to compute the linearized signal at any observed DEB signal  $m_{obs}$ .

The beauty of this method is that it explores the non-linearity in DEB space directly where measurements are made. It also uses data at all the available illuminations. This method shall be our method of choice in future analyses, provided illuminations cover the full dynamic range.

### 3. Analysis Method

All analysis steps were implemented in two Perl scripts: *lincal\_fit* for fitting the FEB ramp fitting at each individual illumination, and *lincalpost\_fit* for fitting to DEB data (derived from the FEB) across all illuminations (see method 2 above). These scripts can only be run from within the WSDS environment.

1. FEB darks that used the “extended source” were collated for each band and median-combined at each SUR sample. For bands 1 and 2, the median-combined FEB darks looked remarkably flat after the first (unreliable) sample. The band 3 and 4 darks showed a small but significant positive gradient. Therefore, darks were only subtracted from the illuminated data for bands 3 and 4.
2. Before fitting the non-linearity model (e.g., Eq. 1), the ramps were “zero-baselined” to avoid fitting an intercept. This involved medianing all the first sample (intercept) values from all repeated exposures at the same illumination, and subtracting this from all samples in all exposures. In the notation of Section 2, the first sample was defined at  $i = 1$  for bands 1 and 2, i.e., to avoid the unreliable sample at  $i = 0$ . For bands 3 and 4, the first sample was defined at  $i = 0$ .
3. As a detail, the band 4 FEB data were first down-sampled by averaging over  $2 \times 2$  pixel blocks in each frame. This will enable the calibration products to be applied to DEB data.
4. All repeated FEB exposures (ramps) at the same illumination were simultaneously fit using a quadratic non-linearity model for every pixel (Eq. 1). The chi-square minimization method described in Section 2 was used. Prior variances ( $\sigma_i^2$ ) for each ramp sample  $y_i$  were computed from the standard deviation across all repeated exposures at each sample  $i$  for the fixed illumination.
5. The chi-square minimization involved a two-pass process. The first pass estimated the fit parameters  $\alpha$  and  $\beta$  and initial estimates of their uncertainties for each pixel. The second pass computed the actual value of the  $\chi^2$  metric (Eq. 2). This was used to check for plausibility of the input data uncertainties  $\sigma_i$ . If these happened to be incorrectly estimated on input, then uncertainties in  $\alpha$ ,  $\beta$  and their covariance will be adversely affected. They therefore need to be adjusted. The  $\chi^2$  was redeemed plausible if its value fell within three standard deviations of its expected value:  $D_F \pm 3\sqrt{2D_F}$ , where  $\langle \chi^2 \rangle = D_F =$  the number of degrees of freedom = number of samples  $- 2$ . If outside this range, then it could indicate the presence of outliers in the data, a bad choice of model, or incorrect prior uncertainties ( $\sigma_i$ ). Spot checks on large numbers of ramps revealed that the choice of model was adequate overall and that outliers were rare. Therefore, if values of  $\chi^2$  were found outside the expected range, the uncertainties in  $\alpha$ ,  $\beta$  (initially from Eq. 4) were re-adjusted as follows:

$$\sigma_{\alpha \text{ or } \beta} \rightarrow \sigma_{\alpha \text{ or } \beta}^{new} = \sigma_{\alpha \text{ or } \beta} \sqrt{\frac{\chi^2}{D_F}}.$$

This is possible because any factors which are used to inflate or deflate the priors  $\sigma_i$  to ensure plausible  $\chi^2$  values can be factored out of the variance formulae for  $\alpha$ ,  $\beta$  in Eq. 4.

6. If we only desire non-linearity coefficients and uncertainties at a single illumination (i.e., as used in the version 1.0 products), then  $C$  and its uncertainty for each pixel are computed using Eqs. 11 and 12.
7. If a refined calibration using method 2 is desired (used for version 2.0+ products), steps 2 to 5 are repeated on FEB data at each illumination. This yields a set of coefficients ( $\alpha$ ,  $\beta$ ) at each illumination. These are then converted to linearized and observed DEB signals ( $m_{lin}$ ,  $m_{obs}$ ) using the formalism under method 2. The set of ( $m_{lin}$ ,  $m_{obs}$ ) pairs are then fit with Eq. 10 to estimate the final effective  $C$ 's and uncertainties for each pixel. To increase the effective DEB dynamic range, the *unsaturated* part of ramps that saturated at or above the 7<sup>th</sup> sample were used in our analysis.
8. Pixels whose non-linearity estimates were abnormally high, very uncertain, or unreliable as determined from bad fits were tagged in a mask.

#### 4. Results Summary

Tables 1 and 2 compare the non-linearity coefficients as estimated using Eq. 11 from *method 1* for the FM and EM electronics. Only “maximal” source apertures (at a single illumination) were used in these analyses, i.e., admitting the largest illumination such that all ramps are still below saturation.

	W1	W2	W3	W4
<b>Temp (K)</b>	31.91	31.86	7.76	7.74
<b>Aperture #</b>	6	6	7	10
<b># Ramps used</b>	20	20	20	10
<b>25<sup>th</sup> %-tile <math>C</math></b>	-7.41e-06	-1.11e-05	-5.10e-06	-6.12e-06
<b>50<sup>th</sup> %-tile <math>C</math></b>	-7.15e-06	-1.03e-05	-4.69e-06	-5.79e-06
<b>75<sup>th</sup> %-tile <math>C</math></b>	-6.90e-06	-9.53e-06	-4.43e-06	-5.63e-06

**Table 1: FM electronics non-linearity coefficients under method 1 ( $C$  from Eq. 11)**

	W1	W2	W3	W4
<b>Temp (K)</b>	32.13	32.15	7.81	7.75
<b>Aperture #</b>	6	6	7	10
<b># Ramps used</b>	10	10	10	10
<b>25<sup>th</sup> %-tile <math>C</math></b>	-7.30e-06	-1.10e-05	-4.84e-06	-5.77e-06
<b>50<sup>th</sup> %-tile <math>C</math></b>	-7.05e-06	-1.02e-05	-4.57e-06	-5.52e-06
<b>75<sup>th</sup> %-tile <math>C</math></b>	-6.80e-06	-9.49e-06	-4.36e-06	-5.39e-06

**Table 2: EM electronics non-linearity coefficients under method 1 ( $C$  from Eq. 11)**



Table 3 compares the percentage non-linearity estimates across all the available apertures (illuminations) using the formalism of *method 2* above. The percentage deviation from non-linearity is defined as:

$$\%NL = 100 * \left( \frac{m_{lin}}{m_{obs}} - 1 \right) \%, \quad (\text{Eq. 17})$$

where  $m_{lin}$  = linearized median DEB pixel signal and  $m_{obs}$  = observed (raw) DEB pixel signal in DN.

Aperture # (~illumination)	W1 %NL; $m_{obs}$	W2 %NL; $m_{obs}$	W3 %NL; $m_{obs}$	W4 %NL; $m_{obs}$
3	0.84; 1621	1.12; 1508	3.36; 3158	10.32; 10767
4	2.03; 3305	2.79; 3084	4.22; 4366	10.37; 11517
5	4.32; 6505	6.16; 6031	5.27; 6392	10.53; 11117
6	10.83; 12302	15.24; 11143	7.23; 10606	10.72; 11455
7	*28.89; *20722	*43.28; *17433	10.57; 18312	10.95; 11855
8	too saturated	too saturated	*19.16; *32037	11.67; 13104
10	too saturated	too saturated	too saturated	13.87; 18429
11	too saturated	too saturated	too saturated	*32.85; *29839

**Table 3: Median percentage deviations from linearity (%NL) at the median observed DEB signals ( $m_{obs}$  in DN) over each array; computed using *method 2* for the FM data. Asterisked numbers (\*) used partial ramps ( $\geq 6$  samples each) due to saturation.**

## 5. Masking Criteria

The mask (msk) image products listed in Section 1 indicate those pixels whose non-linearity estimates were abnormally high, very uncertain, unreliable as determined from bad ramp fits, or NaN'd. These conditions are not mutually exclusive. Thresholds were picked by examining outlying populations in pixel histograms of the non-linearity coefficients, S/N ratios of their estimates, and reduced  $\chi^2$  values.

Below we summarize thresholds for these quantities and the bad-pixel statistics for each band (FM electronics only). Note that only statistics for the active pixel regions are shown. "chi" represents  $\chi^2/\text{dof}$  (i.e., reduced  $\chi^2$ ) where dof = the number of degrees of freedom in the fits (= number of ramp samples from all repeated exposures – 2). The reduced  $\chi^2$  values are compared to those expected for a  $\chi^2$  distribution with the given dof. Coefficient (C) values  $> 0$  are also declared as bad, i.e., significantly positive values (at many sigma) indicate ramps which are "curving upwards".

### Band 1

Number of "active pix" alpha's  $< -2.47993531411339\text{e-}05$  and  $> 0 = 1961$

Number of "active pix" alpha's with S/N  $< 3 = 212$

Number of reduced "active pix" chi-squares  $> 25 = 906$

Number of "active pix" NaN alpha's = 22

**Band 2**

Number of "active pix" alpha's  $< -0.000112862279513593$  and  $> 0 = 3066$

Number of "active pix" alpha's with  $S/N < 3 = 452$

Number of reduced "active pix" chi-squares  $> 65 = 2968$

Number of "active pix" NaN alpha's = 2

**Band 3**

Number of "active pix" alpha's  $< -2.16434583580849e-05$  and  $> 0 = 2302$

Number of "active pix" alpha's with  $S/N < 4 = 16$

Number of reduced "active pix" chi-squares  $> 8 = 2795$

Number of "active pix" NaN alpha's = 14

**Band 4**

Number of "active pix" alpha's  $< -2.58146739392942e-05$  and  $> 0 = 33$

Number of "active pix" alpha's with  $S/N < 6 = 6$

Number of reduced "active pix" chi-squares  $> 2.5 = 970$

Number of "active pix" NaN alpha's = 7

**6. Conclusions**

1. The median percentage deviations from linearity across all bands for a range of DEB signals were summarized in Table 3 for the FM data. At a fiducial DEB signal of 10,000 DN, the non-linearity can be as low as 7% (band 3) and high as 14% (band 2).
2. The bulk of the non-linearity estimates across pixels for each band are significant to least the  $20\text{-}\sigma$  level. Uncertainties were estimated from the repeatability in FEB measurements.
3. The ramp data taken with EM electronics at similar illuminations, but with higher array temperatures (by  $\sim 0.3\text{-}0.5$  K) is more linear by  $\sim 4.5\%$  across all bands. This could be a consequence of the temperature difference. Note that the additional temperature dependent data for the FM set-up (at low and high temperatures) has not yet been analysed.
4. The distribution of the non-linearity across pixels in the active (central) region of each array is  $\sim 4.2\%$ ,  $10\%$ ,  $4.7\%$ , and  $3.6\%$  ( $1\text{-}\sigma$  relative to median  $C$ ) for bands 1, 2, 3, and 4 respectively. Also see "E" histograms in Section 7.
5. Band-2 is our most "non-linear" band. This also has the greatest number of "badly behaving" ramps and not surprisingly, coincides with the greatest number of bad pixels in general.
6. The non-linearity calibration at high DEB signals is weakly constrained by the available FEB lab data. Here, the unsaturated portions of partially saturated ramps were used and thus some additional uncertainty is involved. There is a plan to obtain better sampling of the full dynamic range (albeit coarsely in pixel space) on orbit.

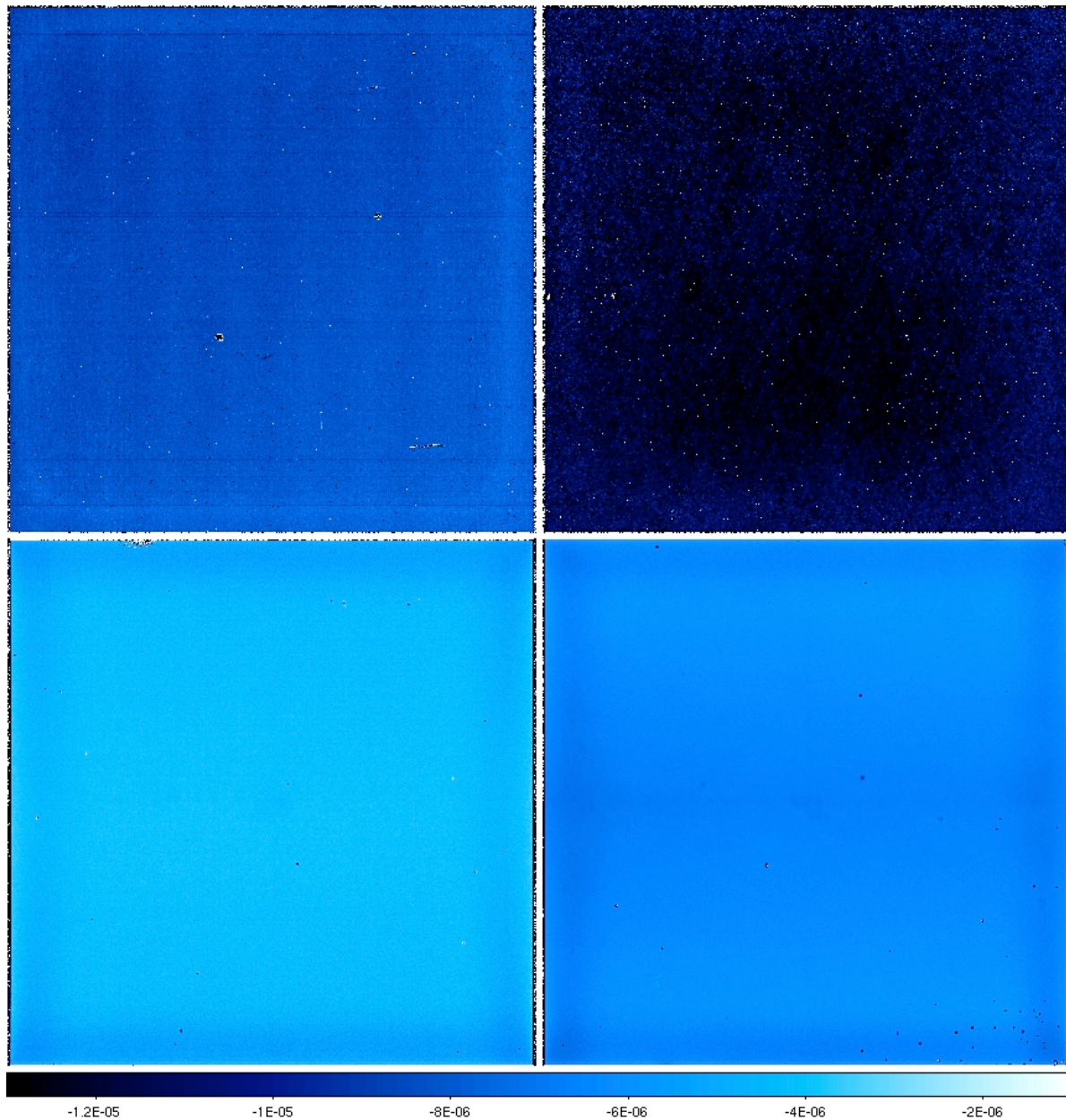


**Figure 1:** Non-linearity calibration coefficient images ( $C$  from Eq. 10 fit to data at all illuminations) for bands 1, 2, 3 and 4: *top left, right; bottom left, right* respectively. Darker regions correspond to greater non-linearity (more negative  $C$ ). All images are at the same stretch.

## 7. Diagnostic Plots

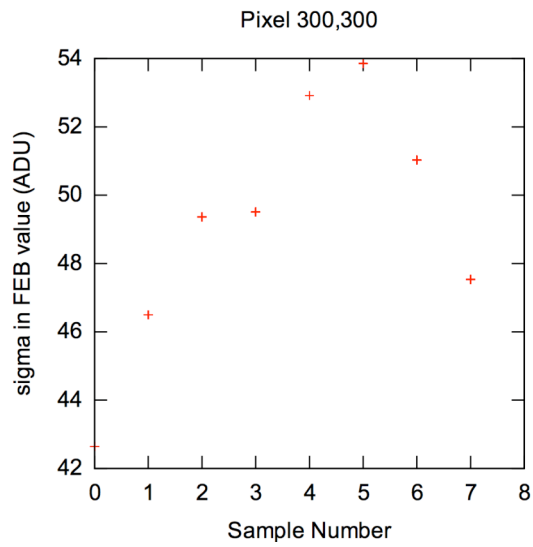
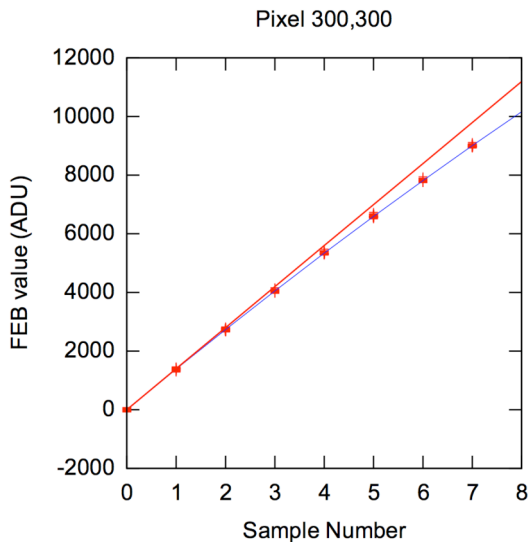
The plots below pertain to analysis of the FM data. Plots from the EM analysis are available upon request. The plots are labelled **A** through **F** for each band. A description is as follows:

- A.** FEB ramp values as a function of sample number for a *single pixel*. Points indicate values from all exposures; blue lines are fits of the quadratic model (Eq. 1), and red lines are the linear component of this fit ( $\beta_i$  in Eq. 1). The ramps have been re-baselined to have zero intercept. Band 1 and 2 ramps were forced start at the second

FEB sample (due to an unreliable first sample) and hence have 8 samples each. The Band 2 plots also show examples of “bad-pixel” ramps (labelled A2 and A3).

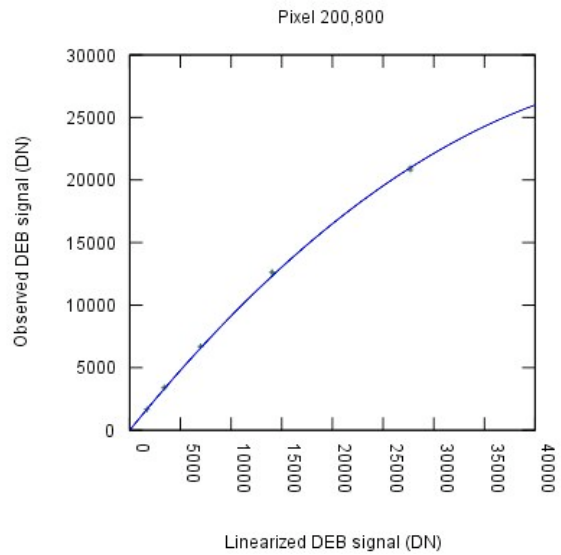
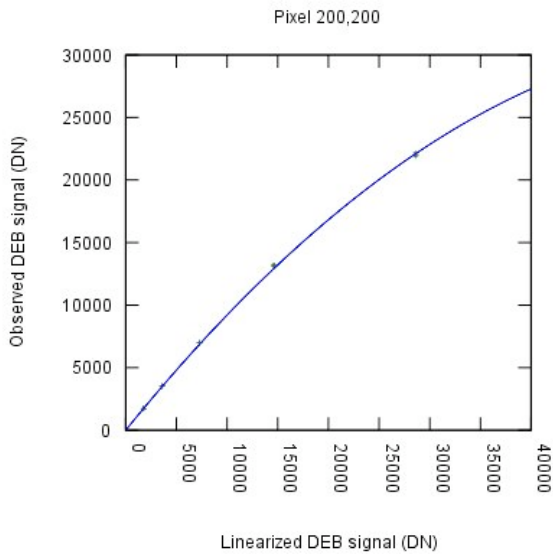
- B.** 1-sigma dispersion in FEB values versus sample number for a single pixel. These were computed from the standard-deviation in FEB values across all repeated exposures at the fixed illumination. Note the increase in these dispersions with sample number for bands 3 and 4. This is due to the increase in Poisson noise along a ramp at the highest illuminations. The effect is not as great as in bands 1 and 2 since these bands are read-noise dominated. As a consequence, a systematically increasing Poisson noise in a ramp implies that the FEB values there will be weighted down in a  $\chi^2$  minimization fit, therefore biasing results. Therefore, inverse variance weighting for the parameter estimation was not used for bands 3 and 4.
- C.** Fit of Eq. 10 to the DEB derived signals ( $m_{lin}, m_{obs}$ ) at all available illuminations for *single pixels*. The DEB signals were derived from fits to the FEB data.
- D.** Predicted linearized DEB signal (in native WISE DN) as a function of observed DEB signal using fits to all illuminations. Blue curves use the 25<sup>th</sup> and 75<sup>th</sup> percentile non-linearity coefficients (top and bottom respectively), and the red curve is for the median non-linearity coefficient over all pixels. The points are median values of ( $m_{lin}, m_{obs}$ ) derived from the available FEB data ( $m_{obs}$  tabulated in Table 3 above).
- E.** Histogram of the non-linearity coefficient for all active-region pixels.
- F.** Histogram of the reduced  $\chi^2$  from fits to the ( $m_{lin}, m_{obs}$ ) DEB-derived data for all active-region pixels.

**Band 1**



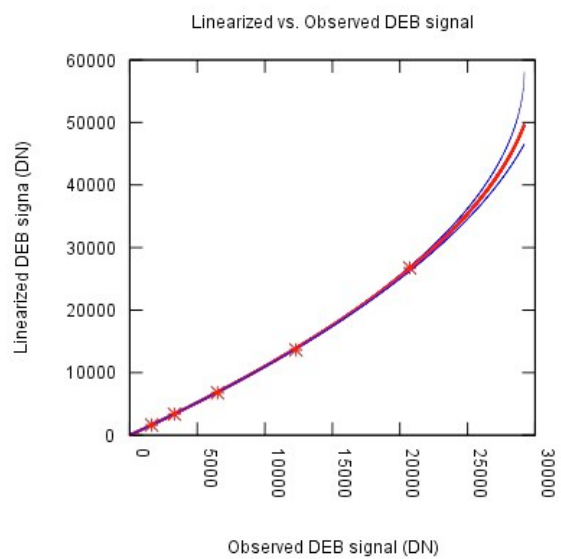
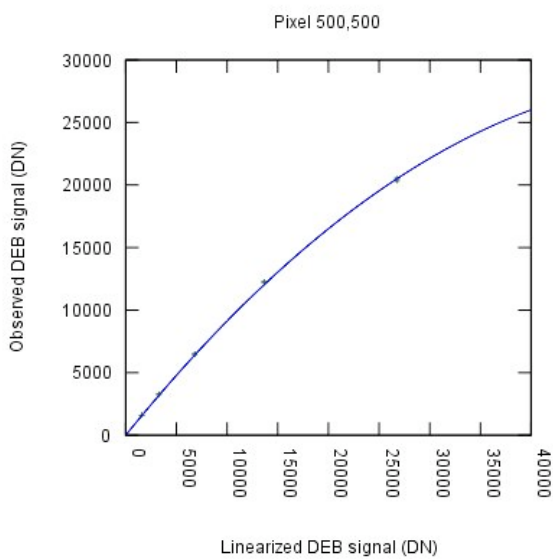
**A**

**B**



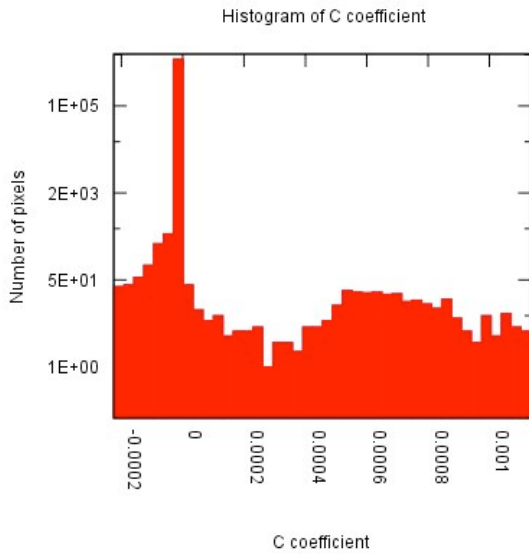
**C**

**C**

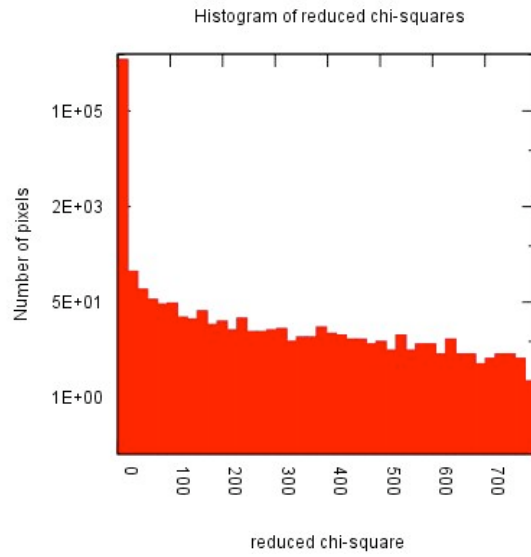


**C**

**D**

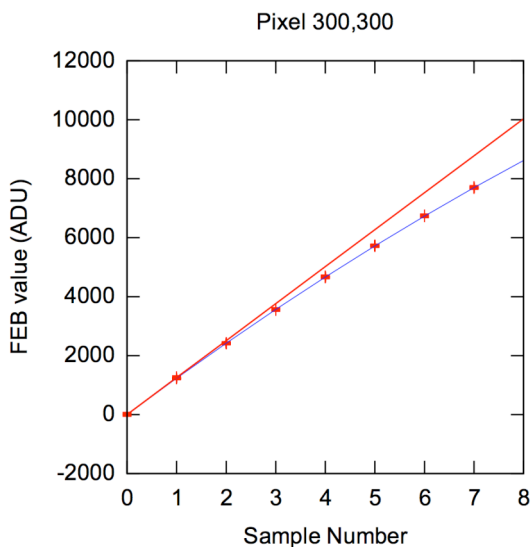


E

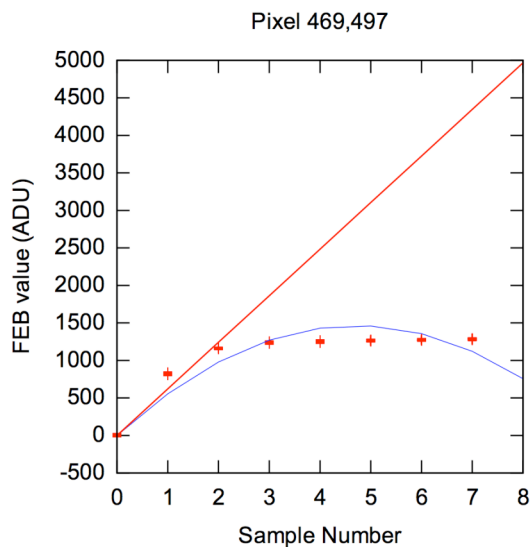


F

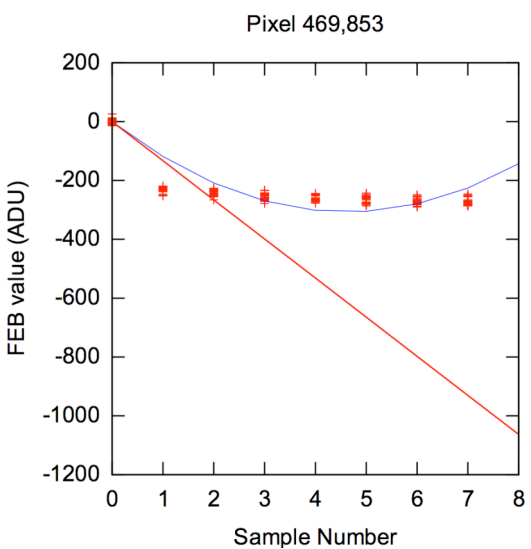
**Band 2**



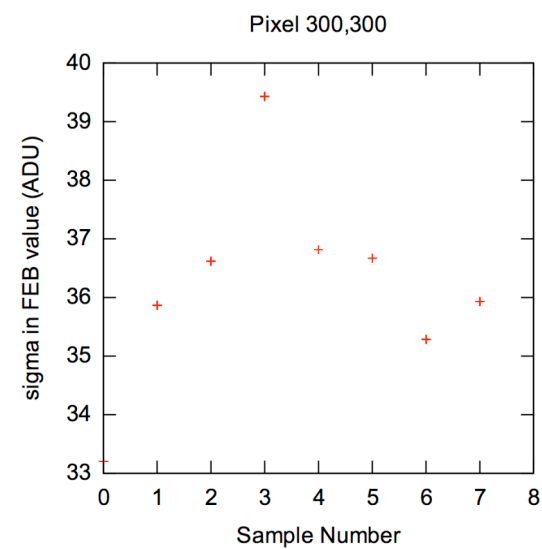
A



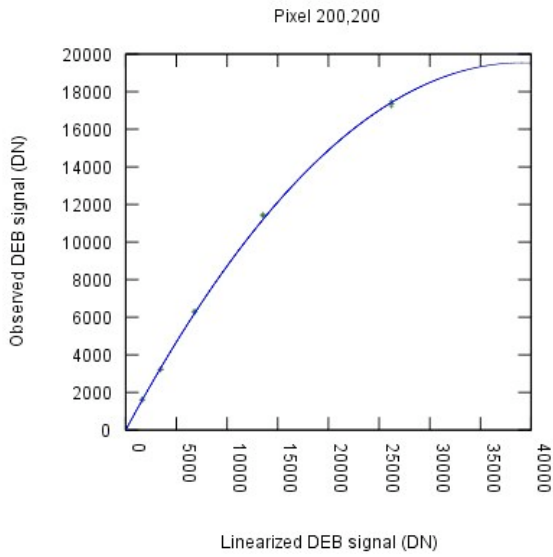
A



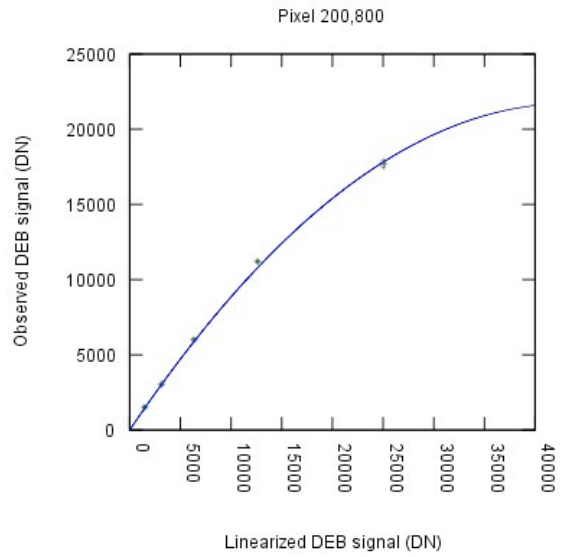
A



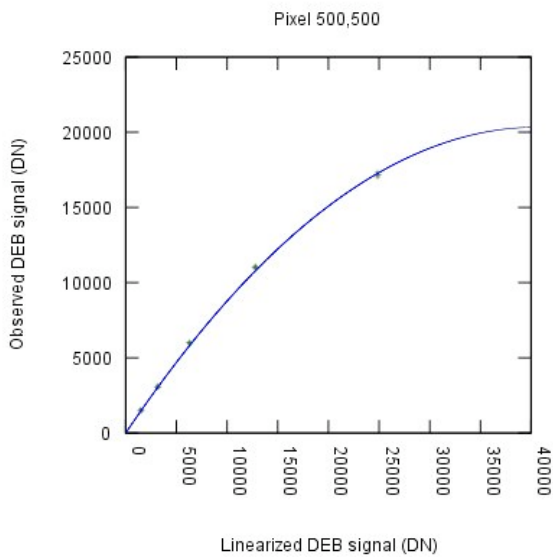
B



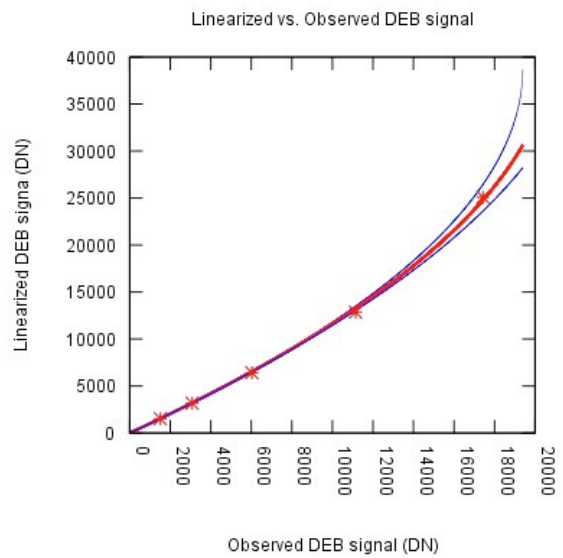
C



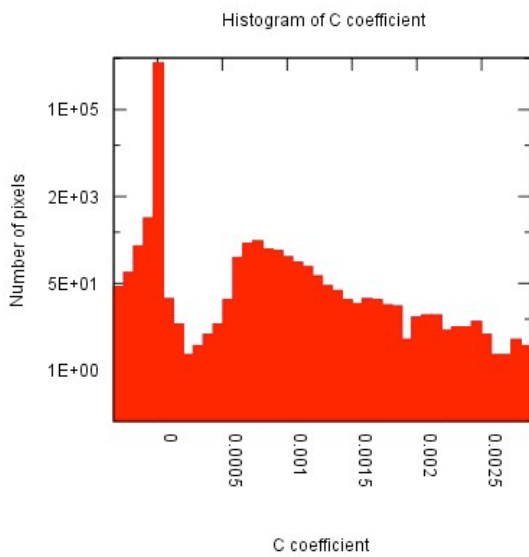
C



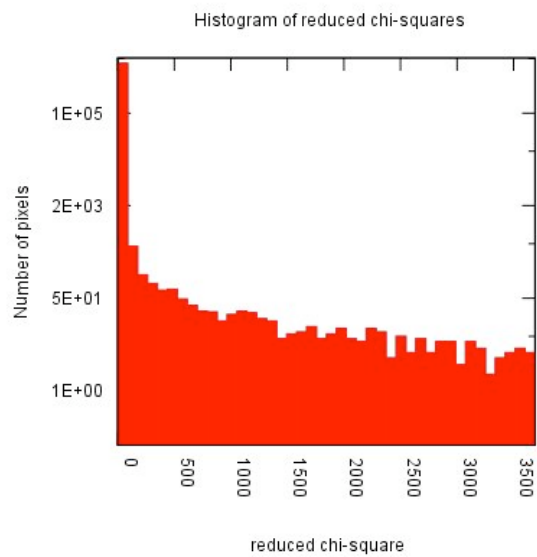
C



D

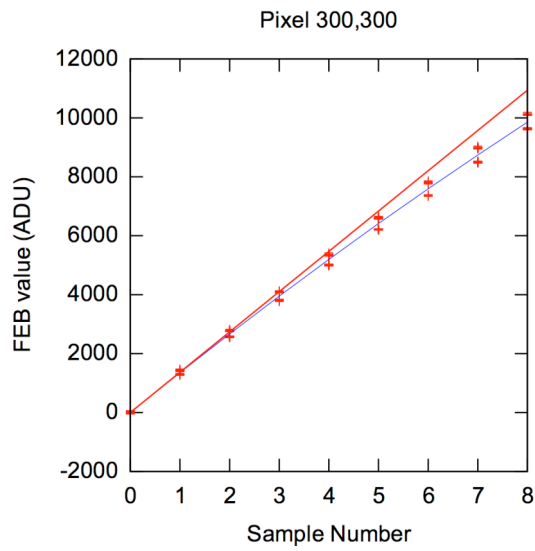


E

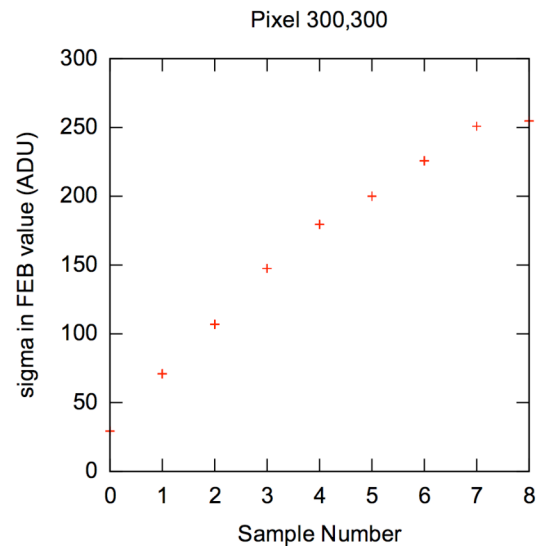


F

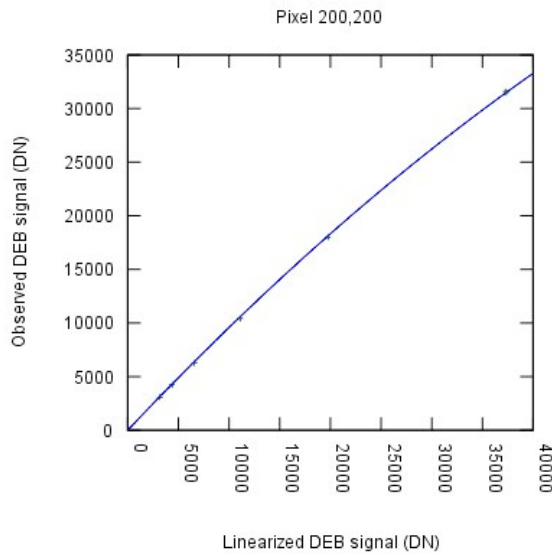
**Band 3**



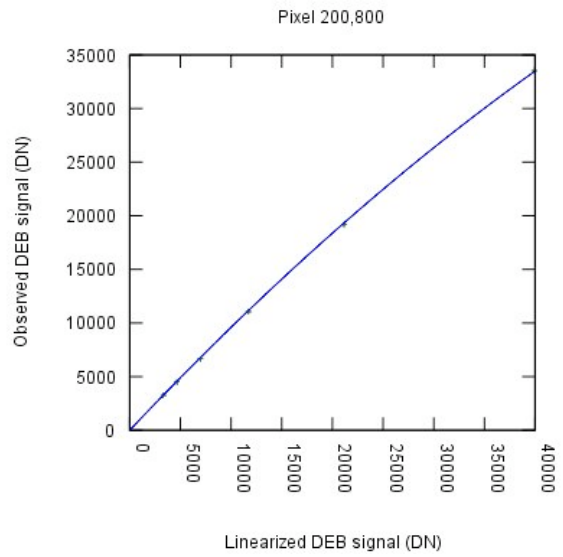
**A**



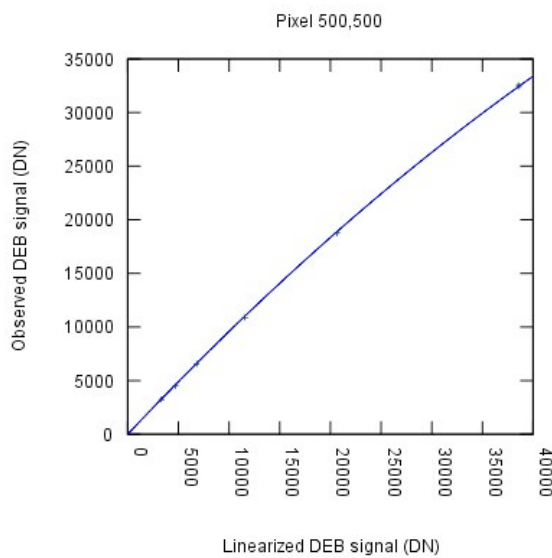
**B**



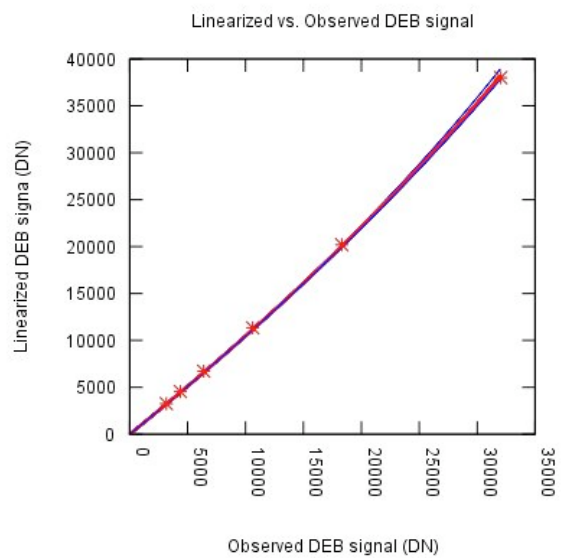
**C**



**C**

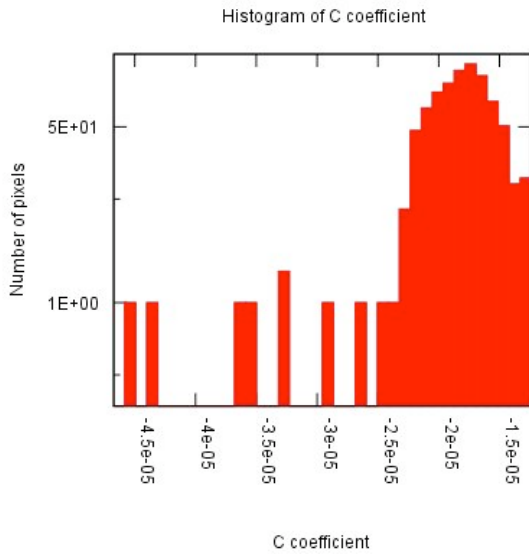


**C**

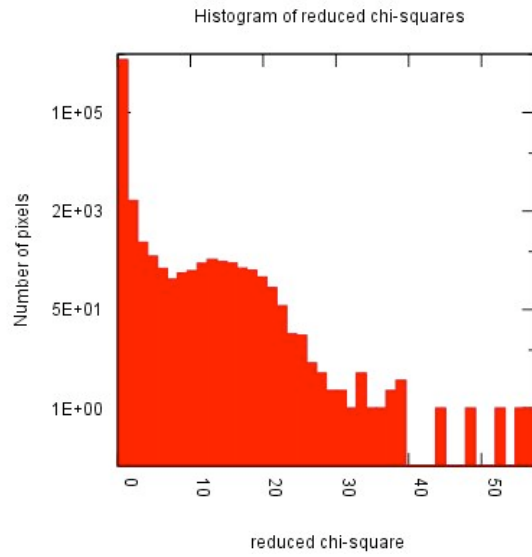


**D**



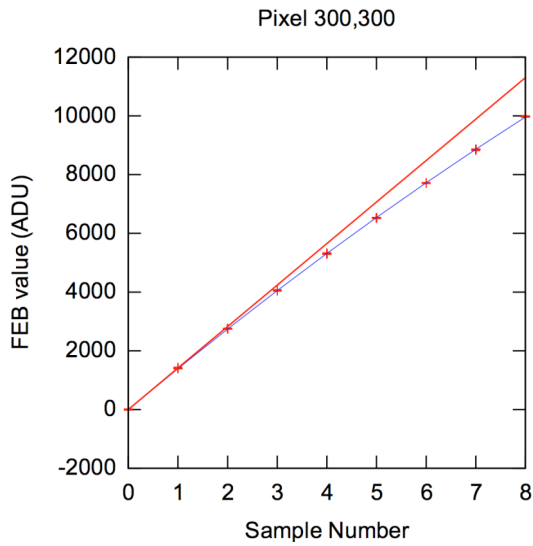


E

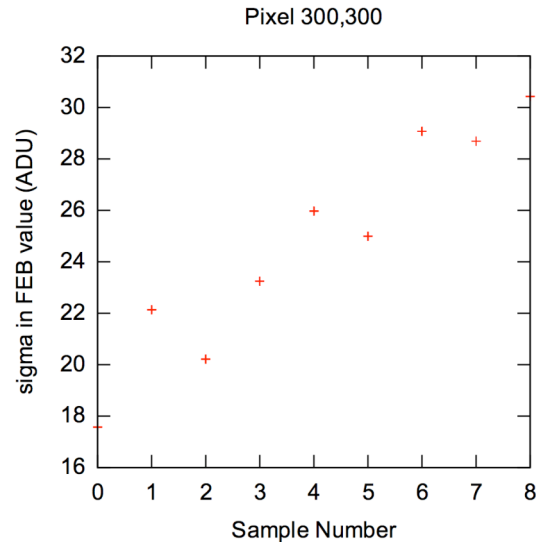


F

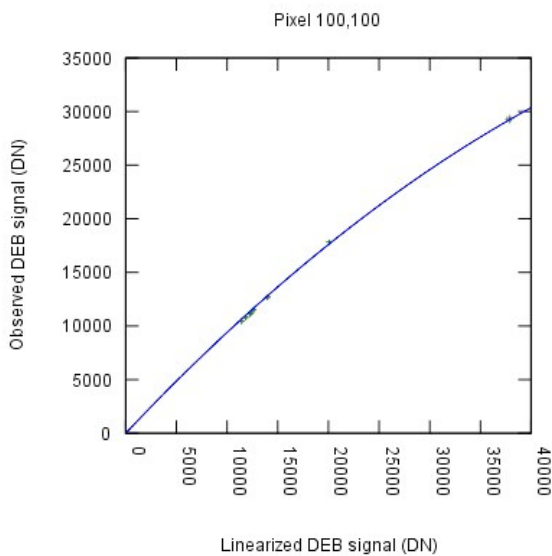
**Band 4**



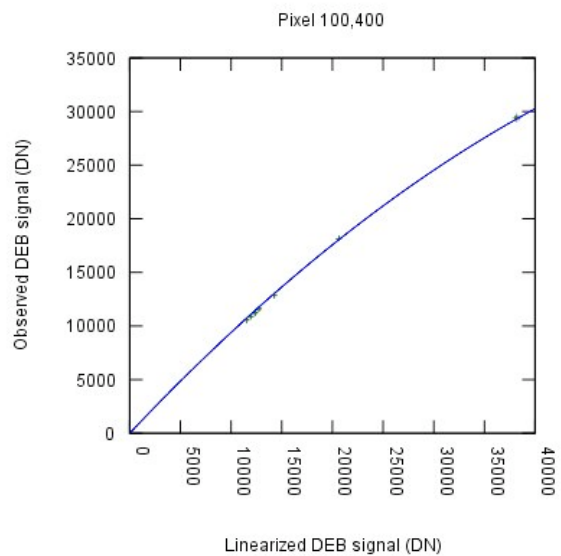
A



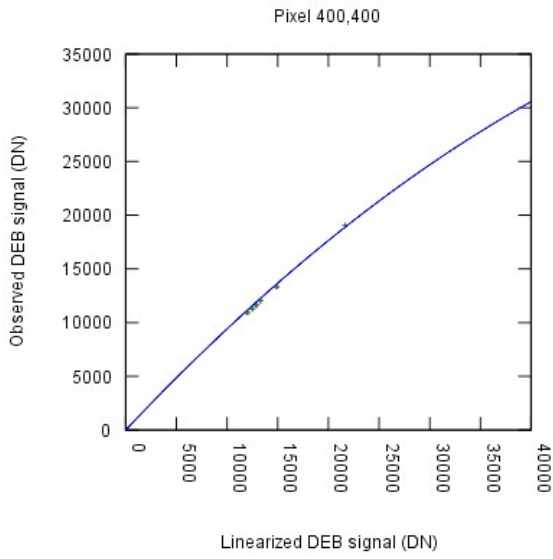
B



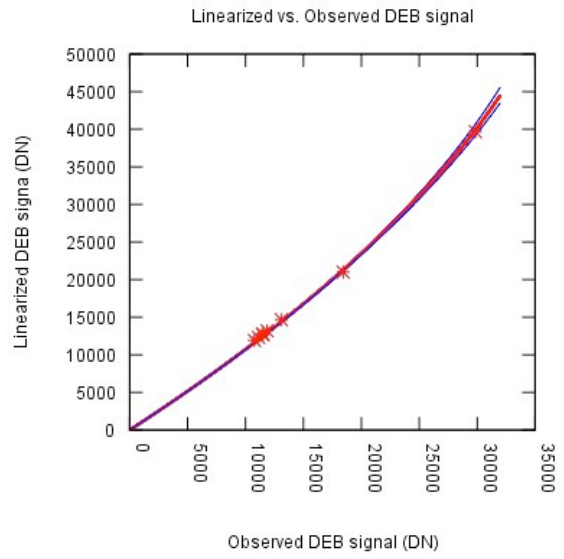
C



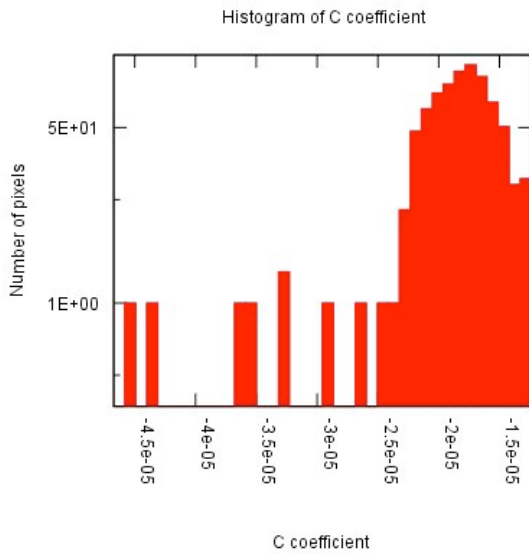
C



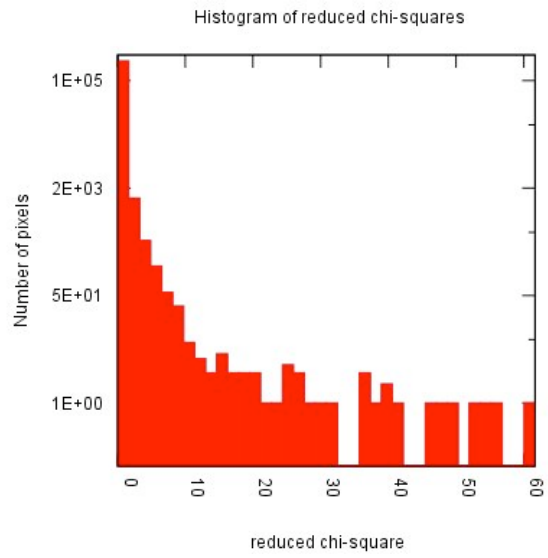
C



D



E



F